Macromolecules

Article

pubs.acs.org/Macromolecules

Aliphatic Polyester Block Polymer Design

Deborah K. Schneiderman and Marc A. Hillmyer*

Department of Chemistry, University of Minnesota, Minneapolis, Minnesota 55455-0431, United States

Supporting Information

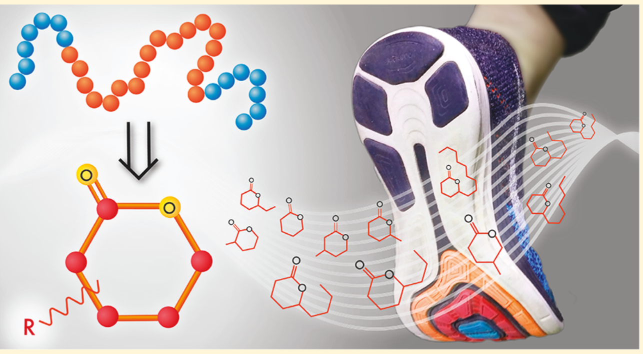

ABSTRACT: Aliphatic polyester block polymers constitute a highly useful and amazingly versatile class of self-assembled materials. Analogous to styrenic block polymers in both design and function, the property profiles of these degradable materials can be precisely tailored by altering the chemical structure of the components. Driven by this ideal, we have examined the impact of *n*-alkyl substituents on the polymerization thermodynamics and kinetics of substituted δ-valerolactone monomers and developed guiding design principles based on critical structure−property relationships in the resulting aliphatic polyesters. Under bulk room temperature conditions the polymerization rate depends strongly on substituent position and exhibits a more modest dependence on alkyl length (from $-CH_3$ to $-(CH_2)_8CH_3$). The enthalpy and entropy of polymerization are significantly influenced by substituent position, but both are largely insensitive to *n*-alkyl length. However, the physical properties of the resulting aliphatic polyesters depend much more on substituent length than on substituent position. Notably, we demonstrate that polymer entanglement molar mass and solubility parameter can be systematically tuned by changing the substituent length. We discuss how these key structure property relationships can be used to inform the design of advanced sustainable materials for future technologies important in the arena of environmentally friendly materials.

INTRODUCTION

Few would argue synthetic polymers are indispensible to modern society. These durable and versatile materials are produced on a scale of hundreds of billions of kilograms annually for many diverse applications, including lightweighting transportation, insulating buildings, and packaging food and pharmaceuticals.[1,2] However, the widespread use of nondegradable, petroleum-derived plastics has created a massive waste management problem and left an indelible mark on the environment.[3,4] Increasingly, public awareness of the problem of plastic pollution has prompted municipal bans on, for example, plastic bags and single-use food packaging.[5,6] An important goal of contemporary polymer science is therefore to create renewable, degradable alternatives that can compete with existing polymers in performance and, perhaps more importantly, cost.

Inspired by the incredible versatility of styrenic ABA triblock polymers, we and others have investigated degradable analogues composed of poly(lactide) (PLA) as the hard "A" blocks and an amorphous aliphatic polyester homopolymer[7−17] or statistical copolymer[18,19] as the soft "B" block. These all-polyester materials are very attractive from a synthetic perspective; because ring-opening transesterification polymerization (ROTEP) is generally very well controlled, the molecular architecture, composition, and molar mass of the block polymer can be easily adjusted to alter the properties of the material.[20] Structural variations in the midblock, such as changes in the substituent size or location, provide another mechanism for tuning the thermal, mechanical, and degradation behavior of the product block polymer.[13,21,22,19]

Although myriad aliphatic lactones with diverse structures have been polymerized, the majority of these monomers have been derived from fossil fuels or from prohibitively expensive natural products.[7,23] Recent advances in synthetic biology have enabled the microbial production of monomers, including lactones, from inexpensive renewable starting materials.[14,24−26] It is important, however, to consider whether the potential value of a new polymer justifies the cost and effort of developing an engineered organism. To help establish general design rules for aliphatic polyester block polymers, we examined how changing the position and size of an alkyl substituent influences lactone polymerizability and resultant polyester properties.

The thermodynamic polymerizability of cyclic monomers is strongly related to ring size.[27] The ring-opening polymerization of small and medium sized cyclic monomers (3−14-membered rings) is typically enthalpically favored ($\Delta H_p^\circ < 0$) but entropically disfavored ($\Delta S_p^\circ < 0$). In practical terms, these thermodynamic characteristics can lead to low equilibrium conversions for monomers characterized by low ring strain. Specific to unsubstituted lactones, experimental and computational studies have revealed that ring strain is highest for β-

Received: January 29, 2016
Revised: February 24, 2016
Published: March 9, 2016

DOI: 10.1021/acs.macromol.6b00211
Macromolecules 2016, 49, 2419−2428

propiolactone (4-membered ring) and much lower for γ-butyrolactone (5-membered ring) and δ-valerolactone (6-membered ring).[28,29] Indeed, the former is nearly incapable of polymerization under typical conditions.[29−32] Although thermodynamic parameters have been reported for the polymerization of several substituted δ-valerolactone monomers, the effect of alkyl substituent size and location on the standard state enthalpy ($\Delta H_\mathrm{p}^\circ$) and entropy ($\Delta S_\mathrm{p}^\circ$) of polymerization has not been experimentally studied in a systematic manner.[14,30,33,34] Importantly, when both $\Delta H_\mathrm{p}^\circ$ and $\Delta S_\mathrm{p}^\circ$ are negative (as is generally true for medium sized lactones), the ratio of the two is proportional to the ceiling temperature (T_c). It is worth noting that T_c, the temperature above which a monomer will not polymerize at a given concentration in a specific solvent, is catalyst independent.

For prospective new monomers, favorable thermodynamics are absolutely necessary but not wholly sufficient; practically, the polymerization must reach high conversion within an operable time. Thermodynamic and kinetic polymerizability are not inherently linked, and the latter is intrinsically dependent on the catalyst used.[35,36] Multitudinous transition metal, enzymatic, and organic catalysts have been developed for the polymerization of lactones.[37−41] When monomer ceiling temperature is low, it is imperative to conduct the polymerization at the lowest temperature and highest monomer concentration practically possible. However, with only few exceptions, kinetic experiments are typically conducted in solution using unsubstituted lactones such as ε-caprolactone or δ-valerolactone.[33,42−45] The effect of alkyl substituent size and location on bulk polymerization rate has not been systematically studied.

In this work we describe the impact of lactone structure on ROTEP of *n*-alkyl substituted δ-valerolactones. Using a series of 12 different δ-lactones, shown in Figure 1, we systematically analyze how changes in the position and length of a substituent influence both $\Delta H_\mathrm{p}^\circ$ and $\Delta S_\mathrm{p}^\circ$. With the same set of monomers, we study how monomer structure impacts the bulk polymerization kinetics. By comparing two different aliphatic polyesters, poly(β-methyl-δ-valerolactone) (**Pβ1**) and poly(δ-pentyl-δ-valerolactone) (**Pδ5**), we also examine how polymer structure can impact key physical characteristics (e.g., solubility parameter (δ) and entanglement molar mass (M_e)). We then discuss how degradable alkyl-substituted polyesters such as these can be used to prepare polyester block polymers suitable for a wide range of potential uses. This comprehensive work melds a fundamental study of lactone polymerizability with an detailed analysis of polymer structure−property relationships to establish guidelines for the design of future sustainable materials that are becoming more and more important for environmentally sound product applications.

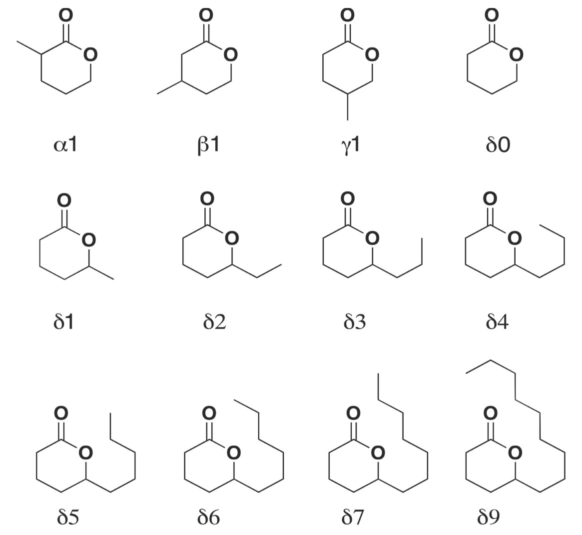

Figure 1. *n*-Alkyl-δ-valerolactone monomers studied in this work. All compounds studied were racemic.

■ RESULTS

The racemic monomers shown in Figure 1 were each polymerized in the bulk at room temperature (~27 °C) with the acid catalyst diphenyl phosphate (DPP). Benzyl alcohol (BnOH) was employed as an initiator to control the molar mass of the polymer. To stop the polymerization, excess triethylamine was added; this deactivates the DPP catalyst but does not appear to have any effect on the resulting polymer structure. Using ^{1}H NMR spectroscopy of quenched aliquots, the initiation and polymerization reactions were independently monitored; this is shown for the monomer **β1** in Figure 2. For this particular monomer, the initiator is fully consumed within minutes while the polymerization approaches equilibrium in a few hours. Although individual monomer structure impacts both initiation and polymerization rates, in all cases we studied the rate of initiation is at least 10 times greater than the rate of propagation.

As shown in the inset of Figure 2c, the initiation reaction is first order in initiator. Initial rate studies, summarized in Table S1 and Figure S60 of the Supporting Information, confirm the polymerization rate increases with both initiator and catalyst concentration. Interestingly, the rate of polymerization does not decrease as monomer is consumed. That is, the slope of monomer conversion over time is linear until the reaction approaches equilibrium. This is atypical for ROTEP polymerizations where, more commonly, the rate of polymerization decreases as the monomer is consumed. A semilogarithmic transformation (Figure S58) of the monomer conversion data in Figure 2 is concave up, indicating the reaction is pseudozero in monomer. The pseudo-zero monomer dependence is also evidenced by the linearity of the data shown in Figure 2c. Although this peculiar observation has not previously reported for DPP-catalyzed polymerizations, it has been observed for other cationic polymerizations where the monomer is more basic than the polymer.[46]

At fixed initial monomer, catalyst, and initiator concentrations, the rate of polymerization is strongly dependent on monomer structure. Among the methyl-substituted lactones, **β1** and **α1** exhibit polymerization rates that are similar to the unsubstituted parent δ-valerolactone (**δ0**) under identical conditions. Among the methyl-substituted monomers, **δ1** is the slowest to polymerize with an observed polymerization rate constant about an order of magnitude smaller than that of the unsubstituted lactone. It is likely that this effect is partially caused by the relatively low reactivity of the propagating secondary alcohol.[47,48] When the substituent position is fixed, increasing the *n*-alkyl length decreases the polymerization rate; however, it is worth noting that the bulk concentration also decreases as the side chain length is increased. On the basis of prior work, we expect a similar trend to hold, even if the polymerizations are conducted in solvent at fixed concentration.[42] Provided the catalyst and initiator loadings are fixed,

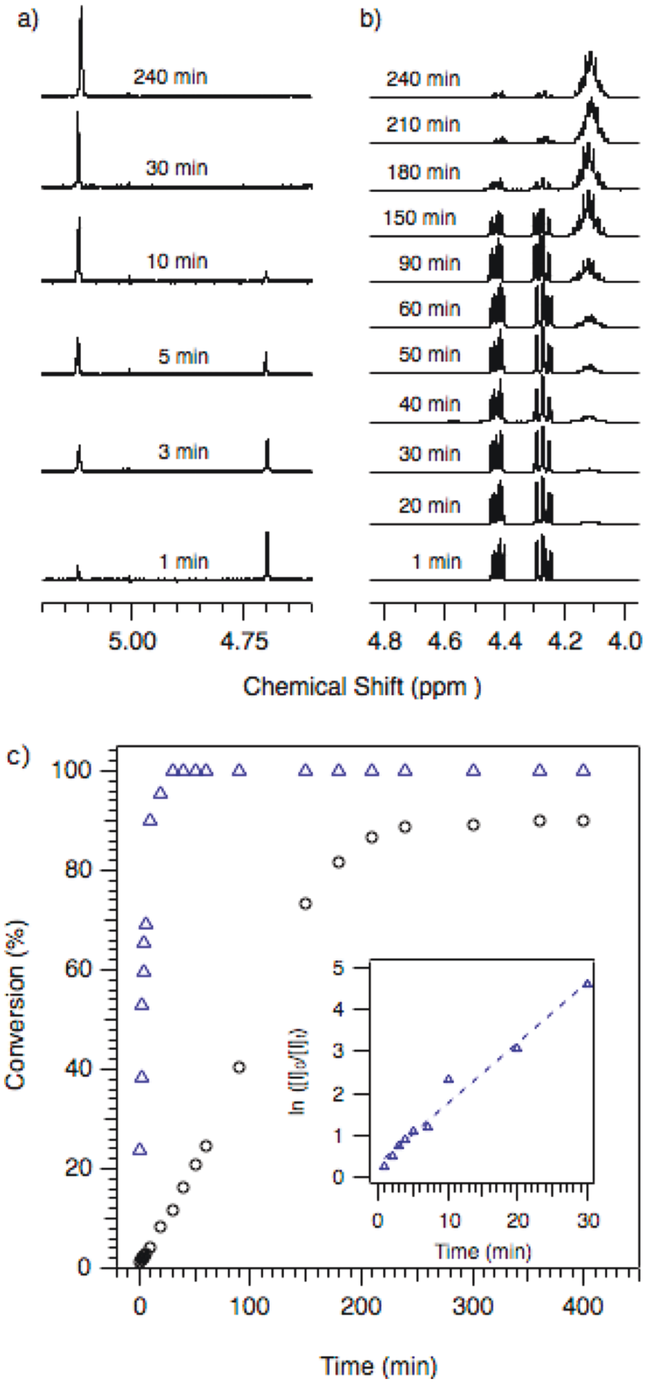

Figure 2. Room temperature (~27 °C) polymerization of $\boldsymbol{\beta}\mathbf{1}$ with $[\mathrm{DPP}]_0 = 0.045$ M, $[\mathrm{BnOH}]_0 = 0.055$ M, and $[\boldsymbol{\beta}\mathbf{1}]_0 = 9.11$ M. (a) ^{1}H NMR spectra overlay showing initiation. The benzyl methylene protons shift from 4.74 ppm in the free alcohol to 5.10 ppm in the initiated polyester. (b) ^{1}H NMR spectra overlay showing monomer consumption. The δ methylene protons, present at 4.25 and 4.40 ppm in the lactone, coalesce and shift to 4.10 ppm in the polyester. Although the chemical shift of the signal(s) corresponding to the δ methine or methylene proton(s) were slightly different for each of the monomers shown in Figure 1, as shown in Supporting Information Figures S1–S21, it was possible to simultaneously monitor both initiation and polymerization by ^{1}H NMR spectroscopy in all cases. (c) Plot of the data in (a) and (b) showing BnOH (△) and $\boldsymbol{\beta}\mathbf{1}$ (○) conversion over time. (inset) Semilogarithmic anamorphosis of BnOH consumption reveals initiation is first-order in initiator concentration.

the observed time required to reach 50% monomer conversion ($t_{1/2}$) allows a more direct comparison of all monomers; these data are summarized in Figure 3 and given in Table S2 of the Supporting Information.

As noted previously, the room temperature kinetics experiments approach an equilibrium monomer concentration ($[\mathrm{M}]_{\mathrm{eq}}$) over time. The residual monomer concentration is highly dependent on substituent location and reaction temperature. Whereas the bulk room temperature polymerizations of $\boldsymbol{\alpha}\mathbf{1}$ and of $\boldsymbol{\gamma}\mathbf{1}$ each approach 98% monomer conversion, the bulk polymerizations of $\boldsymbol{\beta}\mathbf{1}$ and of $\boldsymbol{\delta}\mathbf{1}$ reach lower equilibrium conversion, 91% and 89%, respectively. Within the δ-substituted monomer series, the substituent length influences the equilibrium conversion very little. For all *n*-alkyl substituent lengths the room temperature equilibrium conversion is 89% ± 2%. To learn how monomer structure impacts polymerization thermodynamics, we used the temperature dependence of the equilibrium monomer concentration (i.e., Van't Hoff analysis) to estimate $\Delta H_{\mathrm{p}}^{\circ}$ and $\Delta S_{\mathrm{p}}^{\circ}$. This is shown for the methyl-substituted lactones in Figure 4, where the residual monomer concentration is fit to eq 1:

$$\ln\left(\frac{[\mathrm{M}]_{\mathrm{eq}}}{[\mathrm{M}]_{\mathrm{ss}}}\right) = \frac{\Delta H_{\mathrm{p}}^{\circ}}{RT} - \frac{\Delta S_{\mathrm{p}}^{\circ}}{R} \tag{1}$$

In this expression, T is the temperature at which the polymerization is conducted and $[\mathrm{M}]_{\mathrm{ss}}$ is a standard state monomer concentration. Further discussion and Van't Hoff plots for the other *n*-alkyl-substituted monomers are included in the Supporting Information.

Comparing the methyl-substituted δ-valerolactones, the bulk polymerization of $\boldsymbol{\delta}\mathbf{1}$ is both most exothermic and most entropically unfavored.[14,30] When the *n*-alkyl substituent position is fixed, increasing the length appears to have little effect on the thermodynamics of polymerization. These data are shown in Table 1. Increasing the substituent position from a methyl to a nonyl group produced minor changes in $\Delta S_{\mathrm{p}}^{\circ}$ and $\Delta H_{\mathrm{p}}^{\circ}$. However, the changes are minimal compared to the impact of substituent position. Indeed, we find that within error $\boldsymbol{\delta}\mathbf{7}$ has the same values of $\Delta S_{\mathrm{p}}^{\circ}$ and $\Delta H_{\mathrm{p}}^{\circ}$ as $\boldsymbol{\delta}\mathbf{1}$.

After studying the thermodyanmic and kinetic polymerizability of the lactone monomers, we explored the physical properties of the corresponding poly(esters).

From the plateau modulus of high molar mass (~100 kg mol^{-1}) polymers we estimated the entanglement molar mass of represenative poly(*n*-alkyl-δ-valerolactones); these results are summarized in Table S3. Whereas estimates of the entanglement molar mass (M_{e}) of $\mathbf{P}\boldsymbol{\alpha}\mathbf{1}$ (7.7 kg mol^{-1}) was significantly higher that of PCL (3.0 kg mol^{-1}), the other poly(methyl valerolactones) were all relatively low (4.3, 2.2, and 3.4 kg mol^{-1}, for $\mathbf{P}\boldsymbol{\beta}\mathbf{1}$, $\mathbf{P}\boldsymbol{\gamma}\mathbf{1}$, and $\mathbf{P}\boldsymbol{\delta}\mathbf{1}$, respectively). When the substituent position is fixed, the entanglement molar mass of the polymer increases with substituent length. $\mathbf{P}\boldsymbol{\delta}\mathbf{5}$, for example, has an entanglement molar mass (13.5 kg mol^{-1}) that is about 4 times larger than $\mathbf{P}\boldsymbol{\delta}\mathbf{1}$.

Despite the differences in entanglement molar masses, there were negligible differences in the thermal properties of the *n*-alkyl-substituted poly(δ-valerolactones) studied. Whereas unsubstituted poly(δ-valerolactone) ($\mathbf{P}\boldsymbol{\delta}\mathbf{0}$) is semicrystalline ($T_{\mathrm{m}} = 55$ °C), addition of a methyl substituent is sufficient to disrupt crystallinity in these atactic polymers. Notably, all lactones used in this work are racemic, and the DPP catalyst used is not enantioselective. Addition of the methyl group also increases

DOI: 10.1021/acs.macromol.6b00211
Macromolecules 2016, 49, 2419–2428

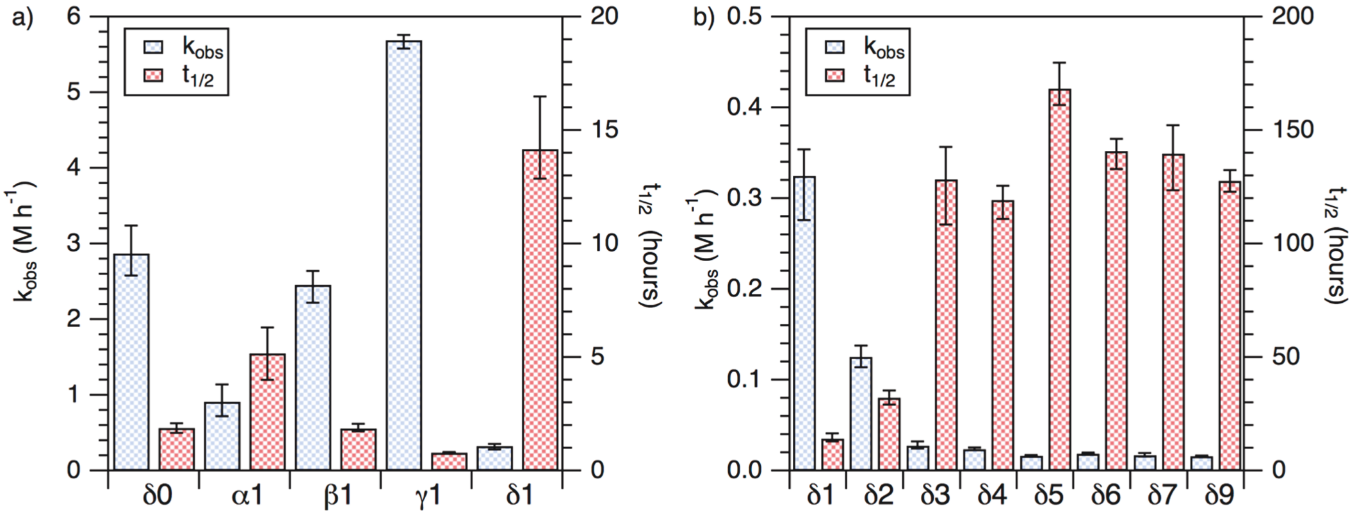

Figure 3. Observed rate for the DPP-catalyzed bulk polymerization of poly(*n*-alkyl-*δ*-valerolactones). The column bars and error bars show the median and range for three samples, respectively, unless otherwise noted. Polymerizations were conducted in the bulk at temperatures of 27 ± 2 °C using initial catalyst and initator loadings of ($[M]_0$:$[DPP]_0 \approx 200{:}1$ and $[M]_0$:$[BnOH]_0 \approx 200{:}1$). The data represented here are provided in Table S2.

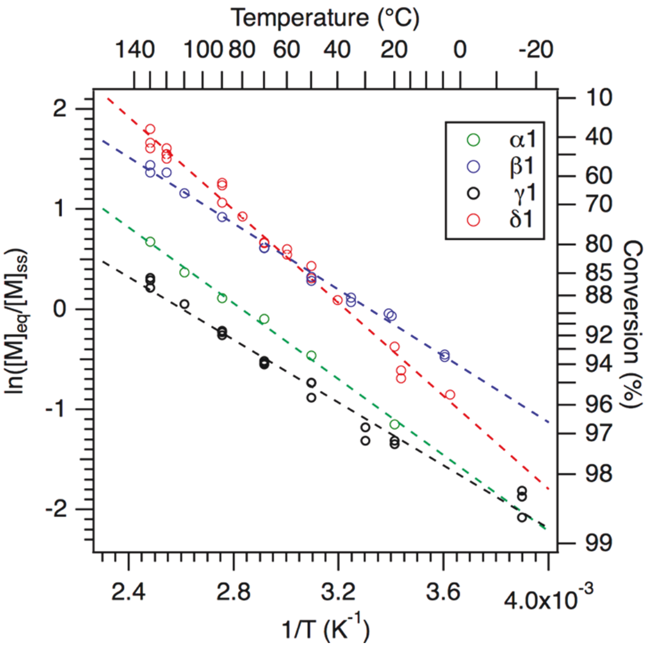

Figure 4. Inverse temperature dependence of $\ln([M]_{eq}/[M]_{ss})$ fit to eq 1. In this work the reference standard state concentration is defined as 1.0 M for convenience. Although it is possible to compare the methyl-substituted monomers directly, this assumption can lead to inaccuracies when comparing monomers with different bulk concentrations. This is further discussed in the Supporting Information. Thermodynamic parameters, ΔH_p° and ΔS_p°, for these and other monomers are summarized in Table 1. The bulk concentrations for the monomers analyzed in this work are given in Table S3.

the glass transition temperature (T_g) slightly (from −60 to −52 °C) as compared to the parent poly(valerolactone). However, as shown in Table S3, there is no significant change in the glass transition temperature when the methyl is replaced with longer *n*-alkyl chains. All of the polymers explored in this work have side chains that are incapable of crystallization at temperatures above the T_g.

Block polymer phase behavior is influenced by a number of factors including the connectivity and volume fractions (f) of the constituent blocks and the segregation strength of the disparate components (χN). Among these parameters the segment−segment interaction parameter, χ, is a property inherent to a given pair of polymers. The interaction parameter is a measure of chemical incompatibility and generally increases with difference in solubility parameters between the two segments. This can be expressed by eq 2:

$$\chi_{A-B} = \frac{V_{ref}(\delta_A - \delta_B)^2}{RT} \tag{2}$$

Here we use estimates of χ and the Hansen solubility parameter of PLA (19.8 J$^{1/2}$ cm$^{-3/2}$) to calculate the solubility parameters of two different polyester midblocks.[62] Because the solubility parameter is independent of a reference volume, it is a convenient metric for comparing structurally dissimilar polymers. In this work we used the assumption that segregation strength at the lamellar to disorder phase boundary is constant ($(\chi N)_{ODT}$ = 17.996 for ABA triblocks) to estimate χ for several compositionally symmetric ABA triblock polymers of different molar masses at the order to disorder transition. N was calculated from the triblock molar mass using a reference volume of 118 Å.[63] The temperature dependence of the segment−segment interaction parameter was fit to eq 3.

$$\chi(T) = \frac{a}{T} + \beta \tag{3}$$

This is shown for PLA-P**δ5**-PLA and PLA-P**β1**-PLA in Figure 5. From these estimates of χ we approximate solubility parameters of 18.4 and 16.8 J$^{1/2}$ cm$^{-3/2}$ for poly(**β1**) and poly(**δ5**), respectively.

It is gratifying to note that the constitutional isomers poly(**β1**) and poly(*ε*-caprolactone) are characterized by the same solubility parameter (18.4 J$^{1/2}$ cm$^{-3/2}$).[64] Poly(**δ5**) has more aliphatic content than poly(**β1**); the solubility parameter of this polymer (16.8 J$^{1/2}$ cm$^{-3/2}$) is actually close to that of polyisoprene.[65] On the basis of group contribution estimates, the solubility parameter is expected to continue to decrease as the length of the side chain increases. However, previous work

Table 1. Summary of the Enthalpy (ΔH_p°) and Entropy (ΔS_p°) of the Ring-Opening Polymerization of Various Lactone Structures

Monomer	ΔH_p° (kJ mol^{-1})	ΔS_p° (J mol^{-1} K^{-1})	^{a}State	References	Monomer	ΔH_p° (kJ mol^{-1})	ΔS_p° (J mol^{-1} K^{-1})	^{a}State	References
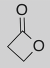	–74 –75 –83	–51 –55 –75	la ^{b}lg lc	49,27 50,49 49	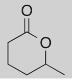	–13.8 –19.3 ± 0.5	–41.2 –62 ± 2	^{g}ss la	30 This work
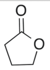	5.1 –5.4	–29 –40	la ^{c}ss	50,51 32	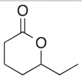	–16.4 ± 0.9	–55 ± 3	la	This work
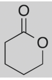	–8.4 –10.5 –27.4	–14.7 –15 –65	^{d}ss lg lc	30 52, 50,30 52,51	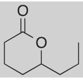	–18.5 ± 0.4	–60 ± 1	la	This work
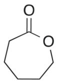	–17.0 –14.0 –13.9	–4 –6 –10.4	lg ^{e}ss la	50,30 30 27	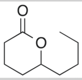	–17.0 ± 0.5	–55 ± 1	la	This work
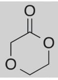	–14.1 –15 to –17 –13.8 ± 0.9	–26.1 –10 to –13 –45 ± 3	la la la	53 54 55,27	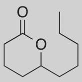	–17.1 ± 0.6 –18.0 ± 0.3	–54 ± 2 –57± 1	la la	33 This work
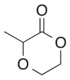	–12.1 ±0.5 –9.9	–42 ± 2 –39.2	^{f}ss la	56 57	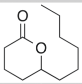	–18.4 ± 0.5	–58 ±2	la	This work
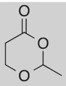	–11.6	–52	la	58	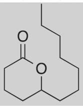	–18.7 ± 0.4	–59 ± 1	la	This work
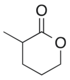	–13.0 ± 0.4	–34 ±1	la	This work	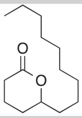	–16.8 ± 0.5	–55 ± 2	la	This work
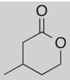	–13.8 ± 0.3	–46 ±1	la	14	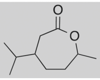	–16.8	–27.4	^{h}ss	59
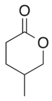	–15.8 ± 0.6	–45 ± 2	la	This work	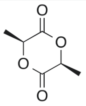	–22.9 –29.1 –23.9	–25.0 –40.7 –43.8	^{i}ss la ^{j}ss	60 60 61

[a] State refers to state of monomer and polymer: a = amorphous state (bulk polymer melt); g = glass, l = liquid monomer, s = solution, c = semicrystalline. [b] This sample, reported as highly elastic, is assumed to be amorphous. [c] CD_2Cl_2, $[M]_0 = 10$ M, these estimates are likely impacted by the formation of a significant proportion of cyclic species. [d] Toluene/DCM (70:30 v/v), $0.2 < [M]_0 < 0.5$ M. [e] Toluene/DCM (70:30 v/v), $[M]_0 = 2.0$ M. [f] Toluene, $[M]_0 = 3.0$ M. [g] Toluene/DCM (70:30 v/v), $1.8 < [M]_0 < 2.0$ M. [h] Toluene $[M]_0 = 0.2$ M. [i] 1,4-Dioxane, $[M]_0 = 1.0$ M. [j] Toluene, $[M]_0 = 1.0$ M.

with styrenic block polymers containing poly(*n*-alkyl methacrylate) midblocks suggests that the value of the solubility parameter may plateau for longer ($n > 10$) side chains.[66−68]

■ DISCUSSION

To maximize monomer conversion in the polymerization of low ceiling temperature monomers, it is necessary to conduct the polymerization at the lowest temperature and highest monomer concentration possible. Therefore, it is important to select a catalyst robust and fast enough at low temperature to catalyze the polymerization without loss of control. In the bulk at room temperature, the DPP catalyst provides excellent control over polymer molar mass and functionality and typically yields polymers with low dispersity values ($Đ \leq 1.20$). Though the DPP-catalyzed polymerization is first-order in monomer when conducted in dilute conditions, it is pseudo-zero-order when conducted the bulk.[42,69,70] Our results are consistent with an activated monomer mechanism where the rate-limiting step is scission of the internal C−O bond of the activated monomer species, as shown in Figure 6. Because the monomer is more basic than the polymer, this mechanism favors polymerization over transesterification.[46]

DPP enables the synthesis of polymers with high control over molar mass and functionality regardless of lactone structure; this is demonstrated in Tables S4 and S6. This high degree of synthetic control is particularly important in the context of block polymers where molecular architecture, composition, and overall molar mass are all intimately linked to the physical properties of the material.[20,63] We found that when the *n*-alkyl substituent is fixed at the *δ*-position, the polymerization rate decreases only slightly as the chain length increases. These results suggest that kinetic considerations do not preclude the polymerization of lactone monomers with arbitrarily long side chains.

All of the substituted monomers we analyzed exhibit ΔH_p° values that are significantly more negative than the value reported for of *δ*-valerolactone (**δ0**). Indeed, for several of the *δ*-substituted monomers the enthalpic drive to polymerize is greater than for the 7-memberd ring monomer *ε*-caprolactone.[50] We expect that minor structural changes (e.g., addition of an alkyl substituent) have a larger influence on the enthalpy

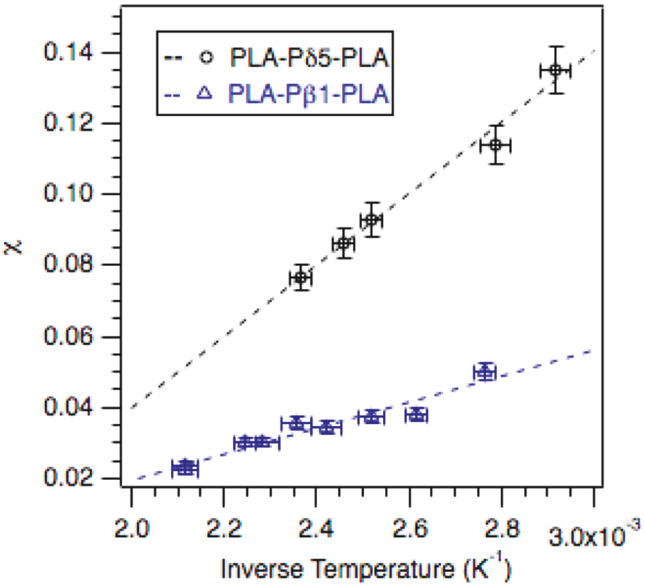

Figure 5. Inverse temperature dependence of $\chi_{\text{PLA-P}\beta 1}$ and $\chi_{\text{PLA-P}\delta 5}$ fit to eq 3. Molecular characterizations of these samples are given in Tables S4−S7. *N* was calculated from the number-average molar mass determined by ^{1}H NMR spectroscopy using a reference volume of 118 Å^3 and room temperature densities of 1.248, 1.10, and 0.97 g cm^{-3} for PLA, **P*β*1**, and **P*δ*5**, respectively. The error in χ is shown as 5% (estimated from the experimental uncertainty in M_n). The T_{ODT} values shown are those determined using dynamic mechanical analysis; error was estimated using the range in the T_{ODT} values measured for the same sample using multiple characterization methods (e.g., SAXS, DMA, and DSC).

of the lactone than on the corresponding polymer. Because ROTEP is an isodesmic reaction, differences in ΔH_p° generally mirror difference in lactone ring strain. It is likely that the higher ring strain of the *n*-alkyl-substituted monomers compared to ***δ*0** is largely due to unfavorable interactions between the alkyl substituents and hydrogen atoms across the ring (transannular strain). In this context it is unsurprising that within the *δ*-substituted monomer series ΔH_p° is essentially constant. Owing to the high conformational freedom of *n*-alkanes, transannular ring strain should remain mostly constant as the substituent length increases. Despite possessing lower ring strain, *δ*-valerolactone actually has a *higher* ceiling temperature than the substituted lactones because its polymerization is less entropically disfavored.

For the substituted monomers studied in this work, polymerization is 2−3 times more entropically disfavored than the polymerization of *δ*-valerolactone. For electronic ground state systems, the change in entropy upon polymerization is the sum of translational, rotational, and vibrational components:

$$\Delta S_p^\circ = \Delta S_{p\,\text{Trans.}}^\circ + \Delta S_{p\,\text{Rot.}}^\circ + \Delta S_{p\,\text{Vib.}}^\circ \tag{4}$$

Gains in rotational and vibrational degrees of freedom can lead to positive changes in ΔS_p° but are only rarely large enough to fully offset the large decrease in translational entropy that usually accompanies polymerization.[71,72] We assume that for *δ*-lactones addition of an alkyl substituent will have a much smaller impact on $\Delta S_{p\,\text{Vib.}}^\circ$ and $\Delta S_{p\,\text{Trans.}}^\circ$ than on $\Delta S_{p\,\text{Rot.}}^\circ$. The addition of a substituent likely decreases the internal rotational freedom of a polymer chain relative to its unsubstituted parent. The rotational freedom of a *δ*-lactone is less influenced by addition of a substituent because for *δ*-valerolactone the small cyclic structure largely prohibits internal bond rotation anyway. At fixed ring size, addition of a substituent therefore tends to decrease ΔS_{rot} relative to an unsubstituted monomer of the same ring size due to restricted rotation in the polymer. The end result is that the addition of substituents to *δ*-valerolactone render the polymerization more thermodynamically unfavorable.

For the specific case of *n*-alkyl *δ*-lactones entropy and enthalpy of polymerization are correlated as shown in Figure S61. This enthalply−entropy compensation behavior, while not unprecedented, presents an interesing dichotomy.[73] To maximize thermodynamic polymerizability, the substituent should be placed in the position that *minimizes* ring strain (an enthalpic phenomena), in this case the *α*-position. This is because the *α* substituent has the least entropically unfavorable impact on the polymerization. The problem of low ceiling temperature could also be avoided by using a substituted seven-membered lactone (e.g., menthide) because polymerization is less entropically disfavored for monomers with larger ring size.[12,59] We note, however, that in the palette of natural lactones five- and six-membered rings are much more prevalent.[74]

We have previously demonstrated using block polymers composed of aliphatic polyesters, e.g. poly(menthide), poly(*ε*-decalactone), and poly(6-methyl-*ε*-caprolactone), that the

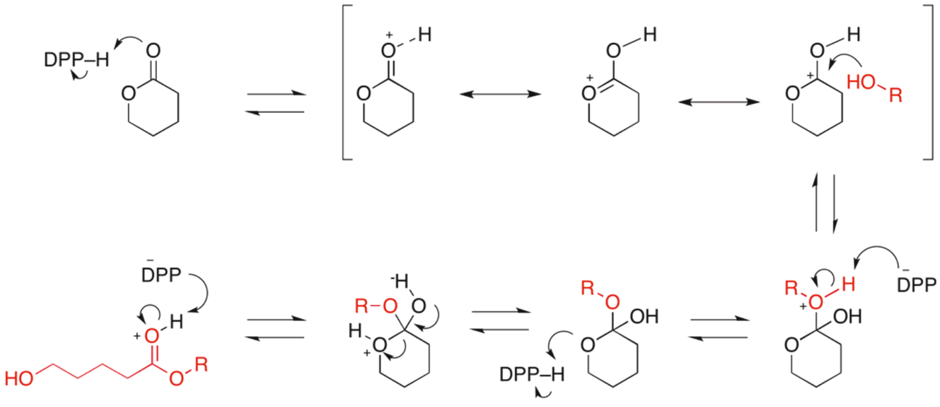

Figure 6. Activated monomer mechanism for the acid-catalyzed polymerization of diphenyl phosphate. ROH (shown above in red) represents the growing polymer chain.

addition of bulky substituents can be used to modify the rheological and mechanical properties of the block polymer.[11,13,59] This tunability is at least partially due to differences in the chain cross section and entanglement molar mass of the soft segment.[22,75,76] The presence of bulky substituents, however, can also lead to an elevation of the glass transition temperature and a concomitant reduction of the service temperature of the elastomer.[77] We have shown in this work that by introducing *n*-alkyl substituents of different sizes it is possible to tune entanglement molar mass without significantly elevating the glass transition temperature.[78]

Modulatuion of aliphatic polyester structure can potentially be used as a tool to design degradable block polymer for a range of specific applications. The methyl-substituted polyesters **Pδ1** and **Pβ1**, for example, are appealing soft blocks for the synthesis of tough plastics and elastomers due to their low entanglement molar masses.[79] The lower modulus of the high entanglement molar mass polymers (e.g., **Pδ5**, poly(menthide), and poly(ε-decalactone)) makes them attractive for use in pressure-sensitive adhesives.[9,80−83] One can easily draw an analogy between these aliphatic polyesters and the low glass transition temperature polydienes currently used in the manufacture of styrenic thermoplastic elastomers. **Pδ1**, for instance, has an entanglement molar mass close to 1,4-polyisoprene, whereas **Pδ5** is more similar to that of poly(ethylethylene) or 1,4-*co*-1,2-polybutadiene.[84] The ability to design polymers with tunable entanglement molar masses also has important implications for processing.

As with entanglement molar mass, the solubility parameters of the aliphatic polyester is also inherent to the structure of the lactone monomer. Although the location of the alkyl substituent has very little effect on polymer polarity, increasing alkyl substituent size causes the polymer to become more hydrophobic. This has important implications for the design of polyester block polymers. For example, while the polarity of the midblock segment can obviously determine solvent resistance, it also directly impacts its compatibility with formulation additives. The latter can indirectly influence characteristics like stability and optical clarity. A more subtle consideration is the interaction between the two blocks. In general, the larger the difference between the solubility parameters of the hard and soft blocks, the larger the magnitude of the Flory−Huggins interaction parameter, χ. Since in this work the hard block is poly(lactide), at a fixed molar mass, decreasing the polarity of the midblock segment effectively increases the segregation strength of the two blocks.[11,13,64,85−89] This is an important characteristic to consider because it dictates the minimum molar mass required for microphase separation to occur, required for desirable mechanical properties, and it also influences practical processing temperatures.

Our studies on δ-lactone polymerizability suggest that to maximize polymerization rate and improve conversion, it is ideal to select a γ-substituted monomers. Although a modest ceiling temperature (315 °C in bulk monomer) may, in general, be considered a synthetic inconvenience, it is possible to leverage this characteristic to facilitate recycling.[32] With regards to polymer design, we note that there is no single perfect polymer; instead, one focuses on matching a material with a specific property profile to the application for which it is best suited. For example, while **Pγ1** may be ideal for the synthesis of tough plastics and elastomers, **Pδ9** may be more suitable for use in pressure-sensitive adhesives.

■ CONCLUSIONS

Our results demostrate that it is both thermodyanmically and kinetically feasible to polymerize substituted δ-valactones with arbitrarily long *n*-alkyl substituents. We have shown that by changing the length of the substituent, the entanglement molar mass and solubility parameter can be modulated without impacting the glass transtion temperature. By understanding synthetic limitations and block polymer structure−property relationships, we show that aliphatic polyesters block polymers can be designed to mirror the properties of commercially relevant styrenic block polymers. These degradable block polymers, sophisticated materials custom-tailored to meet a specific use, are the environmentally friendly plastics of tomorrow.

■ ASSOCIATED CONTENT

Ⓢ Supporting Information

The Supporting Information is available free of charge on the ACS Publications website at DOI: 10.1021/acs.macromol.6b00211.

Materials and methods; detailed synthetic procedures; ^{1}H NMR spectra, DMA data, DSC data, GPC data, and SAXS spectra (Tables S1−S8 and Figures S1−S71) (PDF)

■ AUTHOR INFORMATION

Corresponding Author

*(M.A.H.) E-mail: hillmyer@umn.edu.

Funding

Funding for this work was provided by the Center for Sustainable Polymers at the University of Minnesota, a National Science Foundation (NSF)-supported Center for Chemical Innovation (CHE-1413862). D.K.S. gratefully acknowledges support from the Doctoral Dissertation Fellowship awarded by the University of Minnesota Graduate School.

Notes

The authors declare no competing financial interest.

■ ACKNOWLEDGMENTS

The authors gratefully acknowledge Vigon International and Ortec Inc. for samples of **δ2** and (±)-lactide, respectively. D.K.S. thanks Andrew Mullins for his help translating relevant sections of references written in Russian, Jonathan Hollinger and Marie Vanderlaan for their assistance with SAXS experiments, and Mark Martello, Paula Delgado, and Henry Martinez for helpful and stimulating discussions. D.K.S. and M.A.H. also thank Kiley Schmidt for assistance with TOC artwork. SAXS data were acquired at Sector 12-IDB of the Advanced Photon Source (APS). Additional SAXS experiments were performed at the DuPont−Northwestern−Dow Collaborative Access Team (DND-CAT) Synchrotron Research Center located at Sector 5 of the APS. DND-CAT is supported by the E.I. DuPont de Nemours & Co., The Dow Chemical Company, the U.S. National Science Foundation through Grant DMR-9304725, and the State of Illinois through the Department of Commerce and the Board of Higher Education Grant IBHE HECA NWU 96. Use of the APS was supported by the U.S. Department of Energy, Office of Science, Office of Basic Energy Sciences, under Contract DE-AC02-06CH11357.

■ REFERENCES

(1) Andrady, A. L.; Neal, M. A. Applications and societal benefits of plastics. *Philos. Trans. R. Soc., B* **2009**, *364*, 1977−1984.

(2) PlasticsEurope Plastics−the Facts 2014-20150; http://www.plasticseurope.org/ (accessed Dec 21, 2015).

(3) Thompson, R. C.; Swan, S. H.; Moore, C. J.; vom Sall, F. S. Our plastic age. *Philos. Trans. R. Soc., B* **2009**, *364*, 1973−1976.

(4) Corcoran, P. L.; Moore, C. J.; Jazvac, K. *GSA Today An anthropogenic marker horizon in the future rock record* **2014**, *24*, 4−8.

(5) Romer, J. R.; Tamminen, L. M. Plastic Bag Reduction Ordinances: New York City's Proposed Charge on All Carryout Bags as a Model for U.S. Cities. *Tulane Environ. Law J.* **2014**, *27*, 237−275.

(6) Romer, J. R. The Evolution of SF's Plastic Bag Ban. *Golden Gate Univ. Environ. Law J.* **2007**, *439*, 439−465.

(7) Tsui, A.; Wright, Z. C.; Frank, C. W. Biodegradable Polyesters from Renewable Resources. *Annu. Rev. Chem. Biomol. Eng.* **2013**, *4*, 143−170.

(8) Dijkstra, P. J.; Zhong, Z.; Wim, M.; Feijen, S.; Feijen, J. In *Biorelated Polymers: Sustainable Polymer Science and Technology Springer Science*; Chiellini, E., Gil, H., Braunegg, G., Buchert, J.; Gatenholm, P., van der Zee, M., Eds.; Springer: New York, 2001; Chapter 16, pp 179−194.

(9) Wanamaker, C. L.; Tolman, W. B.; Hillmyer, M. A. Hydrolytic Degradation Behavior of a Renewable Thermoplastic Elastomer. *Biomacromolecules* **2009**, *10*, 443−448.

(10) Wanamaker, C. L.; O'Leary, L. E.; Lynd, N. A.; Hillmyer, M. A.; Tolman, W. B. Renewable-Resource Thermoplastic Elastomers Based on Polylactide and Polymenthide. *Biomacromolecules* **2007**, *8*, 3634−3640.

(11) Martello, M. T.; Hillmyer, M. A. Polylactide-Poly(6-methyl-ε-caprolactone)-Polylactide Thermoplastic Elastomers. *Macromolecules* **2011**, *44*, 8537−8545.

(12) Lin, J. O.; Chen, W.; Shen, Z.; Ling, J. Homo- and Block Copolymerizations of ε-Decalactone with L-Lactide Catalyzed by Lanthanum Compounds. *Macromolecules* **2013**, *46*, 7769−7776.

(13) Martello, M. T.; Hillmyer, M. A.; Schneiderman, D. K. Synthesis and Melt Processing of Sustainable Poly(ε-decalactone)-*block*-Poly(lactide) Multiblock Thermoplastic Elastomers. *ACS Sustainable Chem. Eng.* **2014**, *2*, 2519−2526.

(14) Xiong, M.; Schneiderman, D. K.; Bates, F. S.; Hillmyer, M. A.; Zhang, K. The production of mechanically tunable block polymers from sugar. *Proc. Natl. Acad. Sci. U. S. A.* **2014**, *111*, 8357−8362.

(15) MacDonald, J. P.; Parker, M. P.; Greenland, B. W.; Hermida-Merino, D.; Hamley, I. W.; Shaver, M. P. Tuning thermal properties and microphase separation in aliphatic polyester ABA copolyesters. *Polym. Chem.* **2015**, *6*, 1445−1453.

(16) Olsén, P.; Borke, T.; Odelius, K.; Albertsson, A.-C. ε-Decalactone: A Thermoresilient and Toughening Comonomer to Poly(L-lactide). *Biomacromolecules* **2013**, *14*, 2883−2890.

(17) Ryner, M.; Albertsson, A.-C. Resorbable and Highly Elastic Block Copolymers from 1,5-Dioxepan-2-one and L-Lactide with Controlled Tensile Properties and Hydrophilicity. *Biomacromolecules* **2002**, *3*, 601−608.

(18) Schneiderman, D. K.; Hill, E. M.; Martello, M. T.; Hillmyer, M. A. Poly(lactide)-*block*-poly(ε-caprolactone-*co*-ε-decalactone)-*block*-poly(lactide) copolymer elastomers. *Polym. Chem.* **2015**, *6*, 3641−3651.

(19) Andronova, N.; Albertsson, A.-C. Resilient Bioresorbable Copolymers Based on Trimethylene Carbonate L-Lactide, and 1,5-Dioxepan-2-one. *Biomacromolecules* **2006**, *7*, 1489−1495.

(20) Hillmyer, M. A.; Tolman, W. B. Aliphatic polyester block polymers: renewable, degradable, and sustainable. *Acc. Chem. Res.* **2014**, *47*, 2390−2396.

(21) Pitt, C. G.; Gratzl, M. M.; Kimmel, G. L.; Surles, J.; Schindler, A. Aliphatic Polyesters II. The Degradation of Poly (D,L-lactide), Poly (ε-caprolactone), and Their Copolymers in Vivo. *Biomaterials* **1981**, *2*, 215−220.

(22) Tong, J.-D.; Jerôme, R. Dependence of the Ultimate Tensile Strength of Thermoplastic Elastomers of the Triblock Type on the Molecular Weight between Chain Entanglements of the Central Block. *Macromolecules* **2000**, *33*, 1479−1481.

(23) Yao, K.; Tang, C. Controlled Polymerization of Next-Generation Renewable Monomers and Beyond. *Macromolecules* **2013**, *46*, 1689−1712.

(24) Lu, W.; Ness, J. E.; Xie, W.; Zhang, X.; Minshull, J.; Gross, R. A. Biosynthesis of Monomers for Plastics from Renwable Oils. *J. Am. Chem. Soc.* **2010**, *132*, 15451−15455.

(25) Beller, H. R.; Lee, T. S.; Katz, L. Natural products as biofuels and bio−based chemicals: fatty acids and isopreneoids. *Nat. Prod. Rep.* **2015**, *32*, 1508−1526.

(26) Jambunathan, P.; Zhang, K. Combining biological and chemical approaches for green synthesis of chemicals. *Curr. Opin. Chem. Eng.* **2015**, *10*, 35−41.

(27) Duda, A.; Kowalski, A.; Libiszowski, J.; Penczek, S. Thermodynamic and Kinetic Polymerizability of Cyclic Esters. *Macromol. Symp.* **2005**, *224*, 71−83.

(28) Leitão, M. L.; Pilcher, G.; Meng-Yan, Y.; Brown, J. M.; Conn, A. D. Enthalpies of combustion of γ-butyrolactone γ-valerolactone, and δ-valerolactone. *J. Chem. Thermodyn.* **1990**, *22*, 885−891.

(29) Alemán, C.; Betran, O.; Casanovas, J.; Houk, K. N.; Hall, H. K., Jr. Thermodynamic Control of the Polymerizability of Five-, Six, and Seven-Membered Lactones. *J. Org. Chem.* **2009**, *74*, 6237−6244.

(30) Save, M.; Schappacher, M.; Soum, A. Controlled Ring−Opening Polymerization of Lactones and Lactides Initiated by Lanthanum Isopropoxide, 1 General Aspects and Kinetics. *Macromol. Chem. Phys.* **2002**, *203*, 889−899.

(31) Houk, K. N.; Jabbari, A.; Hall, H. K., Jr.; Alemán, C. Why δ-Valerolactone and γ-Butyrolactone Does Not. *J. Org. Chem.* **2008**, *73*, 2674−2678.

(32) Hong, M.; Chen, E. Completely recyclable biopolymers with linear and cyclic topologies via ring-opening polymerization of γ-butyrolactone. *Nat. Chem.* **2015**, *8*, 42−49.

(33) Martello, M. T.; Burns, A.; Hillmyer, M. Bulk Ring-Opening Transesterification Polymerization of the Renewable δ-Decalactone Using an Organocatalyst. *ACS Macro Lett.* **2012**, *1*, 131−135.

(34) Olsén, P.; Odelius, K.; Albertsson, A.-C. Thermodynamic Presynthetic Considerations for Ring-Opening Polymerization. *Biomacromolecules* **2016**, 10.1021/acs.biomac.5b01698.

(35) Duda, A.; Kowalski, A.; Penczek, S.; Uyama, H.; Kobayashi, S. Kinetics of the Ring-Opening Polymerization of 6-, 7-, 9-, 12-, 13-, 16-, and 17-Membered Lactones. Comparison of Chemical and Enzymatic Polymerizations. *Macromolecules* **2002**, *35*, 4266−4270.

(36) van der Mee, L.; Helmich, F.; de Bruijn, R.; Vekemans, J. A. J. M.; Palamans, A. R. A.; Meijer, E. W. Investigation of Lipase-Catalyzed Ring-Opening Polymerizations of Lactones with Various Ring Sizes: Kinetic Evaluation. *Macromolecules* **2006**, *39*, 5021−5027.

(37) Labet, M.; Thielemans, W. Synthesis of polycaprolactone: a review. *Chem. Soc. Rev.* **2009**, *38*, 3484−38504.

(38) Albertsson, A.-C.; Srivastava, R. K. Recent developments in enzyme-catalyzed ring-opening polymerization. *Adv. Drug Delivery Rev.* **2008**, *60*, 1077−1093.

(39) Kamber, N. E.; Jeong, W.; Waymouth, R. M.; Pratt, R. C.; Lohmeijer, B. G. G.; Hedrick, J. L. Organocatalytic Ring-Opening Polymerization. *Chem. Rev.* **2007**, *107*, 5813−5840.

(40) Lohmeijer, B. G. G.; Pratt, R. C.; Leibfarth, F.; Logan, J. W.; Long, D. A.; Dove, A. P.; Nederberg, F.; Choi, J.; Wade, C.; Waymouth, R. M.; Hedrick, J. L. Guanidine and Amidine Organocatalysts for Ring-Opening Polymerization of Cyclic Esters. *Macromolecules* **2006**, *39*, 8574−8583.

(41) Kiesewetter, M. K.; Shin, E. J.; Hedrick, J. L.; Waymouth, R. M. Organocatalysis: Opportunities and Challenges for Polymer Synthesis. *Macromolecules* **2010**, *43*, 2093−2107.

(42) Zhao, J.; Hadjichristidis, N. Polymerization of 5-alkyl-δ-Lactones catalyzed by diphenyl phosphate and their sequential organocatalytic polymerization with monosubstituted epoxides. *Polym. Chem.* **2015**, *6*, 2659−2668.

(43) Makiguchi, K.; Kikuchi, S.; Yanai, K.; Ogasawara, Y.; Sato, S.; Satoh, T.; Kakuchi, T. Diphenyl Phosphate/4− Dimethylaminopyridine as an Efficient Binary Organocatalyst System for Controlled/Living Ring−Opening Polymerization of L−Lactide Leading to Diblock and End−Functionalized Poly(L−Lactide)s. *J. Polym. Sci., Part A: Polym. Chem.* **2014**, *52*, 1047−1054.

(44) Miranda, M. O.; DePorre, Y.; Vasquez-Lima, H.; Johnson, M. A.; Marell, D. J.; Cramer, C. J.; Tolman, W. B. Understanding the Mechanism of Polymerization of ε-Caprolactone Catalyzed by Aluminum Salen Complexes. *Inorg. Chem.* **2013**, *52*, 13692−13701.

(45) Marlier, E. E.; Macaranas, J. A.; Marell, D. J.; Dunbar, C. R.; Johnson, M. A.; DePorre, Y. Miranda, M. O.; Neisen, B. D.; Cramer, C. J.; Hillmyer, M. A.; Tolman, W. B. *ACS Catal.* **2016**, 10.1021/acscatal.5b02607.

(46) Baśko, M.; Kubisa, P. Cationic Copolymerization of ε−Caprolactone and L,L−Lactide by an Activated Monomer Mechanism. *J. Polym. Sci., Part A: Polym. Chem.* **2006**, *44*, 7071−7081.

(47) Küllmer, K.; Kikuchi, H.; Uyama, H.; Kobayashi, S. Lipase-catalyzed ring-opening polymerization of α-methyl-δ-valerolactone and α-methyl-ε-caprolactone. *Macromol. Rapid Commun.* **1998**, *19*, 127−130.

(48) Kikuchi, H.; Uyama, H.; Kobayashi, S. Lipase-Catalyzed Ring-Opening Polymerization of Substituted Lactones. *Polym. J.* **2002**, *34*, 835−840.

(49) Yevstroprov, A. A.; Lebedev, B. V.; Kulagina, T. G.; Lyudvig, Ye. B.; Belenkaya, B. G. The thermodynamic properties of β-propiolactone, its polymer, and its polymerization in the 0−400 K range. *Polym. Sci. U.S.S.R.* **1979**, *21*, 2249−2256.

(50) Lebedev, B. V.; Estropov, A. A. Thermodynamics of the Polymerization of Lactones. *Dokl. Phys. Chem.* **1982**, *264*, 334.

(51) Duda, A.; Kowalski, A. Thermodynamics and Kinetics of Ring-Opening Polymerization. In *Handbook of Ring-Opening Polymerization*; Dubois, P., Coulembier, O., Raquez, J.-M., Eds.; Wiley-VCH Verlag GmbH & Co. KGaA: Weinheim, 2009; pp 6−7.

(52) Yevstropov, A. A.; Lebedev, B. V.; Kulagina, T. G. Calorimetric study of δ-valerolactone, poly-δ-valerolactone and of the process of polymerization of δ-valerolactone in the 13.8 to 340 K temperature range. *Vysokomol. Soedin., Ser. A* **1982**, *24*, 568−574.

(53) Nishida, H.; Yamashita, M.; Endo, T.; Tokiwa, Y. Equilibrium Polymerization Behavior of 1,4-Dioxan-2-one in Bulk. *Macromolecules* **2000**, *33*, 6982−6986.

(54) Lebedev, B. V.; Bykova, T. A.; Kiparisova, E. G.; Belen'kaya, B. G.; Filatova, V. N. Thermodynamics of p-dioxanone, of its polymerization and of poly(p-dioxanone) at 0−450 K. *Vysokomol. Soedin., Ser. A Ser. B* **1995**, *37*, 187−196.

(55) Libiszowski, J.; Kowalski, A.; Szymanski, R.; Duda, A.; Taquez, J. M.; Degée, P.; Dubois, P. Monomer-Linear Macromolecules-Cyclic Oligomers Equilibria in the Polymerization of 1,4-Dioxan-2-one. *Macromolecules* **2004**, *37*, 52−59.

(56) Bechtold, K.; Hillmyer, M. A.; Tolman, W. B. Perfectly Alternating Copolymers of Lactic Acid and Ethylene Oxide as a Plasticizing Agent for Polylactide. *Macromolecules* **2001**, *34*, 8641−8648.

(57) Lochee, Y.; Jhurry, D.; Bhaw-Luximon, A.; Kalangos, A. Biodegradable Poly(ester-ether)s: ring-opening polymerization of D,L-3-methyl-1,4-dioxan-2-ones using various initiator systems. *Polym. Int.* **2010**, *59*, 1310−1318.

(58) Neitzel, A. E.; Petersen, M. A.; Kokkoli, E.; Hillmyer, M. A. Divergent Mechanistic Avenues to an Aliphatic Polyesteracetal or Polyester from a Single Cyclic Esteracetal. *ACS Macro Lett.* **2014**, *3*, 1156−1160.

(59) Zhang, D.; Hillmyer, M. A.; Tolman, W. B. Catalytic Polymerization of a Cyclic Ester Derived from a "Cool" Natural Precursor. *Biomacromolecules* **2005**, *6*, 2091−2095.

(60) Duda, A.; Penczek, S. Thermodynamics of L-Lactide Polymerization. Equilibrium Monomer Concentration. *Macromolecules* **1990**, *23*, 1636−1639.

(61) Wang, Y.; Hillmyer, M. A. Synthesis of Polybutadiene-Polylactide Diblock Copolymers Using Aluminum Alkoxide Macroinitiatiors. Kinetics and Mechanism. *Macromolecules* **2000**, *33*, 7395−7403.

(62) Schively, M. L.; Coonts, B. A.; Renner, W. D.; Southard, J. L.; Bennet, A. T. Physico-chemical characterization of a polymeric injectable implant delivery system. *J. Controlled Release* **1995**, *33*, 237−243.

(63) Matsen, M. W. Effect of Architecture on the Phase Behavior of AB-Type Block Copolymer Melts. *Macromolecules* **2012**, *45*, 2161−2165.

(64) Schneiderman, D. K.; Hill, E. M.; Martello, M. T.; Hillmyer, M. A. Poly(lactide)-*block*-poly(ε-caprolactone-co-ε-decalactone)-*block*-poly(lactide) copolymer elastomers. *Polym. Chem.* **2015**, *6*, 3641−3651.

(65) Grulke, E. A. In *Polymer Handbook*, 4th ed.; Brandrup, J., Immergut, E. H., Grulke, E. A., Eds.; John Wiley & Sons Inc.: 1999.

(66) Wang, S.; Robertson, M. L. Thermodynamic Interactions between Polystyrene and Long−Chain Poly(n-Alkyl Acrylates) Derived from Plant Oils. *ACS Appl. Mater. Interfaces* **2015**, *7*, 12109−12118.

(67) Lewin, J. L.; Maerzke, K. A.; Schulz, N. E.; Ross, R. B.; Sipmann, J. I. Prediction of Hildebrand solubility parameters of acrylate and methacrylate monomers and their mixtures by molecular simulation. *J. Appl. Polym. Sci.* **2010**, *116*, 1−9.

(68) Wang, S.; Kesava, S. V.; Gomez, E. D.; Robertson, M. L. Sustainable Thermoplastic Elastomers Derived from Fatty Acid. *Macromolecules* **2013**, *46*, 7202−7212.

(69) Makiguchi, K.; Satoh, T.; Kakuchi, T. Diphenyl Phosphate as an Efficient Cationic Organocatalyst for Controlled/Living Ring-Opening Polymerization of δ-Valerolactone and ε-Caprolactone. *Macromolecules* **2011**, *44*, 1999−2005.

(70) Makiguchi, K.; Ogasawara, Y.; Kikuchi, S.; Satoh, R.; Kakuchi, T. Diphenyl Phosphate as an Efficient Acidic Organocatalyst for Controlled/Living Ring−Opening Polymerization of Trimethylene Carbonates Leading to Block, End−Functionalized, and Macrocyclic Polycarbonates. *Macromolecules* **2013**, *46*, 1772−1782.

(71) Manzini, B.; Hodge, P.; Ben-Haida, A. Entropically−driven ring−opening polymerization of macrocyclic esters with up to 84−membered rings catalyzed by polymer−supported Candida antarctica. *Polym. Chem.* **2010**, *1*, 339−346.

(72) Sawada, H. Thermodynamics of Polymerization. 1. *J. Macromol. Sci., Polym. Rev.* **1969**, *3*, 313−396.

(73) Kałużyński, K.; Penczek, S. Anionic Polymerization of 2-Oxo-1,2,3 λ5-dioxaphosphorinane. Thermodynamics. *Makromol. Chem.* **1979**, *180*, 2289−2293.

(74) Shilna, I.; Nakata, K. Medium-Sized Lactones. In *Natural Lactones and Lactams: Synthesis, Occurrence and Biological Activity*; Janecki, T., Ed.; Wiley: Weinheim, Germany, 2014; pp 193−227.

(75) Vincent, P. I. A correlation between critical tensile strength and polymer cross-sectional area. *Polymer* **1972**, *13*, 558−560.

(76) Dobkowski, Z. Determination of Critical molecular weight for entangled macromolecules using the tensile strength data. *Rheol. Acta* **1995**, *34*, 578−585.

(77) Yu, J. M.; Dubois, P.; Jerome, R. Synthesis and Properties of Poly(isobornyl methacrylate (IBMA)-*b*-butadiene (BD)-*b*-IMBA Copolymers: New Thermoplastic Elastomers of a Large Service Temperature Range. *Macromolecules* **1996**, *29*, 7316−7322.

(78) Fetters, L. J.; Lohse, D. J.; Milner, S. T.; Graessley, W. W. Packing Length Influence in Linear Polymer Melts on the Entanglement, Critical, and Reptation Molecular Weights. *Macromolecules* **1999**, *32*, 6847−6851.

(79) Kanai, H.; Sullivan, V.; Auerbach, A. Impact Modification of Engineering Thermoplastics. *J. Appl. Polym. Sci.* **1994**, *53*, 527−541.

(80) Daoulas, K. C.; Theodorou, D. N. Experimental and Self−Consistent−Field Theoretical Study of Styrene Block Copolymer Self-Adhesive Materials. *Macromolecules* **2004**, *37*, 5093−5109.

(81) Shin, J.; Lee, Y.; Tolman, W. B.; Hillmyer, M. A. Pressure-Sensitive Adhesives from Renewable Triblock Copolymers. *Macromolecules* **2011**, *44*, 87−94.

(82) Sangjun, L.; Lee, K.; Kim, Y.-W.; Shin, J. Preparation and Characterization of a Renewable Pressure−Sensitive Adhesive System Derived from ε-Decalactone, L-Lactide, Epoxidized Soybean Oil, and Rosin Ester. *ACS Sustainable Chem. Eng.* **2015**, *3*, 2309−2320.

(83) Kraus, G.; Rollmann, K. W. The Entanglement Plateau in the Dynamic Modulus of Rubbery Styrene−Diene Block Copolymers. Significance to Pressure−Sensitive Adhesive Formulations. *J. Appl. Polym. Sci.* **1977**, *21*, 3311−3318.

(84) Fetters, L. J.; Lohse, D. J.; Richter, D.; Witten, T. A.; Zirkel, A. Connection between Polymer Molecular Weight, Density, Chain Dimensions, and Melt Viscoelastic Properties. *Macromolecules* **1994**, *27*, 4639−4647.

(85) Lee, I.; Panthani, T. R.; Bates, F. S. Sustainable Poly(lactide-b-butadiene) Multiblock Copolymers with Enhanced Mechanical Properties. *Macromolecules* **2013**, *46*, 7387−7398.

(86) Wolf, J. H.; Hillmyer, M. A. Ordered Nanoporous Polycyclohexylethylene. *Langmuir* **2003**, *19*, 6553−6560.

(87) Schmidt, S. C.; Hillmyer, M. A. Morphological Behavior of Model Poly(ethylene-alt-propylene)-b-Polylactide Block Polymers. *J. Polym. Sci., Part B: Polym. Phys.* **2002**, *40*, 2364−2376.

(88) Lee, S.; Gillard, T. M.; Bates, F. S. Fluctuations, order, and disorder in short diblock copolymers. *AIChE J.* **2013**, *59*, 3502−3513.

(89) Zalusky, A. S.; Olayo-Vales, R.; Wolf, J. H.; Hillmyer, M. A. Ordered Nanoporous Polymers from Polystyrene-Polylactide Block Copolymers. *J. Am. Chem. Soc.* **2002**, *124*, 12761−12773.